J Appl Electrochem (2007) 37:1085–1091
DOI 10.1007/s10800-007-9360-y

ORIGINAL PAPER

# A parametric study of a platinum ruthenium anode in a direct borohydride fuel cell

**N. Duteanu · G. Vlachogiannopoulos ·**
**M. R. Shivhare · E. H. Yu · Keith Scott**

Received: 19 January 2007 / Revised: 25 June 2007 / Accepted: 29 June 2007 / Published online: 20 July 2007

**Abstract** Data on the performance of a direct borohydride fuel cell (DBFC) equipped with an anion exchange membrane, a Pt–Ru/C anode and a Pt/C cathode are reported. The effect of oxidant (air or oxygen), borohydride and electrolyte concentrations, temperature and anode solution flow rate is described. The DBFC gives power densities of 200 and 145 mW cm$^{-2}$ using ambient oxygen and air cathodes respectively at medium temperatures (60 °C). The performance of the DBFC is very good at low temperatures (ca. 30 °C) using modest catalyst loadings of 1 mg cm$^{-2}$ for anode and cathode. Preliminary data indicate that the cell will be stable over significant operating times.

**Keywords** Direct borohydride fuel cell · Platinum ruthenium anode · Anion exchange membrane · Fuel cell

## 1 Introduction

The interest in fuel cells and progress towards commercialisation has accelerated recently due to an increase in availability of practical fuel cell systems and their increased cost competitiveness, both for transportation and for stationary power generation. For portable and small scale applications low temperature fuel cells are favoured due to safety concerns and the need for quick start and thermal insulation requirements [1–3]. Current system development is focusing on a range of fuels including methanol and hydrogen with increasing interest in the use of sodium borohydride. Sodium borohydride can either be converted catalytically to hydrogen which is used in the fuel cell or alternatively may be used directly. The attractions of borohydride are that it is a fuel that is easily stored and distributed, chemically stable in highly alkaline media and non-combustible. In the DBFC the following reactions occur:

$$\text{Anode}: BH_4^- + 8OH^- = BO_2^- + 6\,H_2O + 8e^- \quad E^0 = -1.24\,\text{V (vs. SHE)} \tag{1}$$

$$\text{Cathode}: 2O_2 + 4H_2O + 8e^- = 8OH^- \quad E^0 = 0.4\,\text{V (vs. SHE)} \tag{2}$$

$$\text{Overall}: BH_4^- + 2O_2 = BO_2^- + 2H_2O \quad E^0 = 1.64\,\text{V} \tag{3}$$

Attractions of the DBFC are its high theoretical open circuit voltage of 1.64 V and its high energy density of 9285 Wh (kg $NaBH_4$)$^{-1}$; which are 0.4 V and 3,200 Wh kg$^{-1}$ higher than those of direct methanol fuel cells [3]. Therefore, borohydride has been proposed as an alternative fuel to hydrogen, which has issues with its use, such as anode poisoning (when reformate is the fuel), supply, storage and transportation [3], and to other organic fuels, which have problems of lower activity, capacity and oxidation efficiency [1, 4, 5].

As the cost of fuel cells that use polymer membranes is still too high in comparison to more conventional power generators, research into new and cost-effective membranes is very active [6]. The early DBFC, e.g. a $KBH_4/O_2$ fuel cell, used an asbestos separator and could only use dilute fuel, e.g. 2 wt.% [7]. The high electrical resistance of the asbestos made it unsuitable for further use in DBFC.

N. Duteanu · G. Vlachogiannopoulos · M. R. Shivhare ·
E. H. Yu · K. Scott (✉)
Chemical Engineering and Advanced Materials, University of Newcastle upon Tyne, Merz Court, Newcastle upon Tyne NE1 7RU, UK
e-mail: k.scott@newcastle.ac.uk

A recently developed DBFC adopted an anion conducting membrane, which gave maximum power densities of 20 and 63 mW cm$^{-2}$ at ambient temperature and 70 °C respectively [8]. The negative effect of borohydride crossover from the anode chamber to the cathode was identified and Nafion® cation membranes were used as alternatives [9, 10], which led to higher power densities, e.g. 160 mW cm$^{-2}$ at 300 mA cm$^{-2}$ and 70 °C [11]. A possible concern with the use of Nafion® cation membranes is the accumulation of sodium hydroxide in the cathode pores which may precipitate and also lead to carbonate precipitation due to the presence of carbon dioxide in air. Consequently, the membrane material of choice would ideally be an anion exchange membrane with minimal crossover of borohydride.

A second major factor in the development of the DBFC is that of obtaining a suitable anode material that is electrochemically active for borohydride oxidation but does not catalyse the hydrolysis of borohydride to hydrogen in the fuel cell. The latter factor would result in a significant loss in fuel efficiency and energy generation ability. Anodes which have been considered for borohydride fuel cells include Pt, Au, Ni and metal hydrides. In this work we consider the use of a binary alloy of Pt and Ru deposited on carbon.

## 2 Experimental

The following materials and chemicals were used as received: $RuCl_3$ (99%, Aldrich), $H_2PtCl_6$ (99.9%, Janssen), $NaBH_4$ (99%, Fisher), NaOH (99.99%, Aldrich), Nafion solution (5 wt.%, Aldrich), carbon powder (Vulcan XC-72R, Cabot), Ketjen-300J carbon black (Akzo Nobel), carbon paper (Toray, TGPH120, E-TEK), Nafion® 117 membrane (DuPont), Pt mesh (20 cm$^2$, 99.99%, Goodfellow) and $Hg/Hg_2SO_4$ (saturated $K_2SO_4$) reference electrode (MMS, Russell). Deionised water (ELGASTAT B124 Water Purification Unit, The Elga group) and high purity gases $N_2$ and $O_2$ (BOC) were used.

### 2.1 MEA preparation

Membrane electrode assemblies (MEA) were prepared by bonding anode and cathode catalyst layers to opposite sides of a polymer electrolyte membrane and covering the catalyst layers with carbon paper based current collectors (or gas distributors). The membrane used was an anion exchange polymer electrolyte (ADP—Morgane, Solvay S.A.). Table 1 gives properties of the ADP—Morgane membrane at 25 °C [12]. Before fabrication of the MEA the membrane was rinsed with de-ionised water and dried.

**Table 1** Basic properties of ADP—Morgane membrane

| Material | Cross-linked fluorinated polymer |
|---|---|
| Exchange group | Quaternary ammonium |
| Thickness fully humidified (μm) | 150–160 |
| Resistance (in 0.6 M NaCl) (Ω cm$^2$) | 1.5–4.5 |
| Resistance (in 1 M NaOH) (Ω cm$^2$) | 0.5 |
| Maximum operational temperature (°C) | 55 |
| Working pH | 0–10 |

The catalyst electrodes were made from ink prepared by mixing isopropyl alcohol (IPA) with 10% Nafion and carbon supported catalyst. Carbon supported Pt–Ru (60 wt.%—ETEK, USA) and carbon supported Pt (60 wt.%—ETEK, USA) were used for the anode and cathode catalyst layer, respectively. Nafion was used as the binder, as a solubilised form of the anion exchange membrane was not available. Nafion has a proven ability to act as a binder in PEM fuel cells, especially when low pressing temperatures are required, as in this work. In this context it is preferable to PTFE. In electrode preparation the catalyst layer was sprayed on top of one gas diffusion electrode. The desired amount of catalyst was 1 mg cm$^{-2}$ for both electrodes. The gas diffusion electrode consisted of a micro porous layer (Ketjen black carbon, with 10% PTFE) sprayed on top of a carbon paper (20 wt.% wet-proofed Toray 90 carbon paper, ETEK USA). After electrode preparation, the membrane was sandwiched between the anode and cathode and hot pressed together at 50 kg cm$^{-2}$ for 3 min at 80 °C.

### 2.2 Fuel cell tests

In assembling the DBFC, the anode and cathode of the MEA were in contact with high-density graphite blocks (Ralph Coidan), impregnated with phenolic resin, into which gas/liquid flow channels were machined. The ridges between the channels provided the electrical contact to the carbon electrodes and the total machined geometrical area of 4 cm$^2$ was taken as the active area of the cell. Copper sheets contacted the graphite blocks as current collectors. Electrical heaters were mounted at the rear of the Cu plates to maintain the desired cell temperature, which was controlled through a temperature controller and monitored by thermocouples buried in the graphite blocks. Conditioning of the MEAs were carried out by passing water through both chambers at 40 °C for 10 h and then using a 1.0 mol dm$^{-3}$ (M) NaOH solution in the anode chamber for 5 h. After conditioning, the anode was supplied with a solution of sodium borohydride in sodium hydroxide and the cathode with either air or oxygen.

Once the cell voltage had decayed to a steady value, polarisation curves were recorded in galvanostatic mode, starting from the open circuit potential and moving to higher current densities. Anode polarisation curves were measured with respect to a hydrogen fed cathode acting both as a reference electrode and a counter electrode. Cathode polarisation data were derived by subtracting electrode polarisation values from the respective cell polarisation data at various current densities [13, 14]. Other details of MEA fabrication, fuel cell assembly and operation are reported elsewhere [15].

## 3 Results and discussion

### 3.1 Influence of temperature

The effect of temperature on the direct borohydride fuel cell performance was explored between 30 and 60 °C. This temperature range was chosen to reflect both the anticipated operating temperature of the DBFC in portable and certain mobile applications and to minimise any membrane degradation at higher temperatures. Other operating variables were maintained constant, unless otherwise stated, at the following values: borohydride concentration 1.0 M in 1.0 M sodium hydroxide; anode solution feed rate 2.78 $cm^3$ $min^{-1}$, cathode flow rate 0.4 $cm^3$ $min^{-1}$, without back pressure, i.e. approximately zero bar (gauge).

Figure 1 shows that an increase in temperature is beneficial to anode polarisation, i.e. higher potentials are achieved at a fixed current density. The anode potentials fall significantly, at a fixed current density, with increasing temperature as a result of improved borohydride oxidation kinetics [15] and increased mass transport [13, 16]. In addition, as temperature was increased, the conductivities of NaOH and $NaBH_4$ increased, which also had a favourable influence on anode performance.

The anode polarisation curves showed some unusual characteristics, which were consistently obtained with several MEAs used in this study. These have been observed with other anode catalysts studied in the Newcastle laboratories. Results of this latter work will be reported later. It can be seen (Fig. 1) that the curves exhibit what is effectively a point of inflection at potentials around 150–200 mV, which might suggest some mass transport limitation. However the data do not correspond to a mass transport limitation in borohydride or hydroxide ion flux. One possibility was in situ production of hydrogen gas by borohydride hydrolysis. However no significant quantities of hydrogen gas were observed from the anode, even at higher current densities. Cell tests which fed hydrogen gas, as a two-phase mixture with the hydroxide solution, directly into the cell did not give anode polarisation characteristics obtained with the DBFC (Fig. 1). The observed anode characteristics probably reflect the complex mechanism of borohydride oxidation and understanding the anode characteristics is the subject of on-going work.

Figure 2 shows Tafel plots of the anode polarisation data in the low overpotential region, i.e. up to a current density of 100 mA $cm^{-2}$. The values of the kinetic parameters obtained from this data are given in Table 2. Assuming a transfer coefficient of 0.5 the data suggest that a one-electron transfer step in the oxidation is rate controlling. Considering the characteristics of the anode

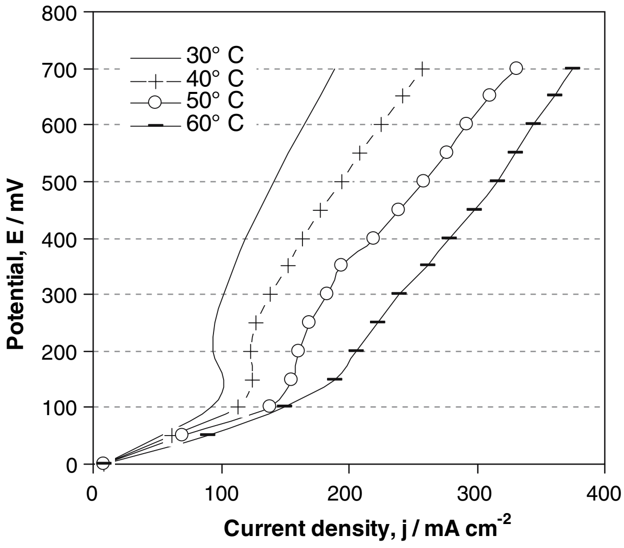

**Fig. 1** Effect of temperature on anode polarisation. Borohydride concentration 1.0 M in 1.0 M sodium hydroxide; solution anode flow rate 2.78 $cm^3$ $min^{-1}$, cathode flow rate 0.4 $cm^3$ $min^{-1}$, without back pressure

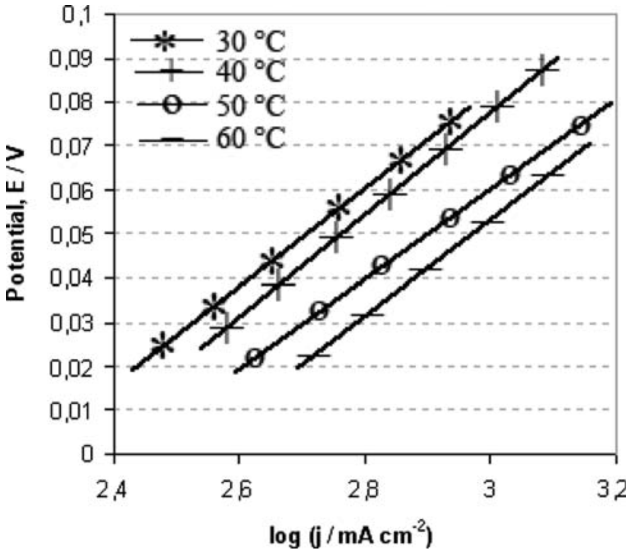

**Fig. 2** Tafel plots of borohydride ion oxidation in the DBFC. Borohydride concentration 1.0 M in 1.0 M sodium hydroxide; solution anode flow rate 2.78 $cm^3$ $min^{-1}$

**Table 2** Kinetic parameters for borohydride oxidation

| Temperature (°C) | Tafel slope (V $dec^{-1}$) | log ($j_0$/A $m^{-2}$) | $j_0$/A $m^{-2}$ |
|---|---|---|---|
| 30 | 0.11 | 2.26 | 180 |
| 40 | 0.14 | 2.39 | 243 |
| 50 | 0.12 | 2.46 | 288 |
| 60 | 0.12 | 2.54 | 346 |

polarisation curves, we expected to see similar behaviour reflected in the cell polarisation and power density curves. This behaviour was indeed seen in the data, as shown in Fig. 3, which gives the cell polarisation and power density curves obtained at different temperatures. It is significant that even though Nafion® was used as a binder good power performance was achieved. The binder clearly held the supported catalyst together and apparently did not appear to significantly impede $OH^-$ or $BH_4^-$ ion transport. This behaviour is likely to be due to the relatively thin Nafion layer formed over the catalyst, which enables reasonable ionic diffusion. In addition Nafion exhibits good solubility for oxygen which also assists in achieving good power densities.

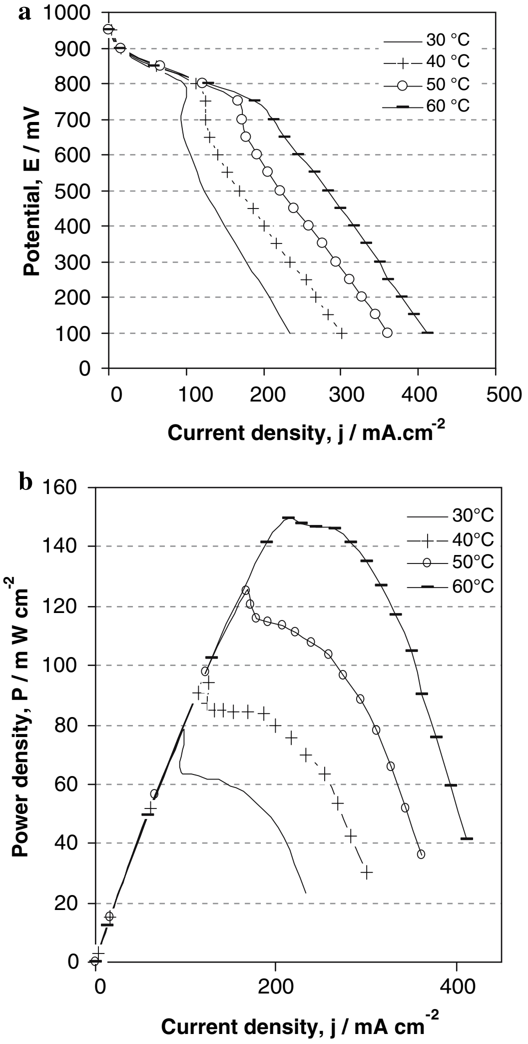

**Fig. 3** Cell polarisation and power density for an oxygen fed DBFC. (**a**) Cell polarization, (**b**) Power density behaviour. Borohydride concentration 1.0 M in 1.0 M sodium hydroxide; solution anode flow rate 2.78 $cm^3$ $min^{-1}$, cathode flow rate 0.4 $cm^3$ $min^{-1}$, without back pressure

As shown in Fig. 3, the cell polarisation curves started at an open circuit potential of 950 mV, which is much lower than the theoretical value predicted from standard potentials. This behaviour is due to a combination of several factors; the reduced concentrations of borohydride and hydroxide ions and oxygen due to the Nafion thin film, borohydride crossover and interfacial effects at the electrocatalyst interfaces. The variation in cell potential with current density showed a similar behaviour to that obtained for the anode polarisation (Fig. 1). There were essentially two linear regions of cell potential versus current density with a change in slope at around 750 mV.

In terms of cell polarisation the increase in temperature had an overall positive effect giving higher cell potentials and also peak power densities. The maximum peak power density was close to 150 mW $cm^{-2}$ using oxygen. Values of peak power density are given in Table 3 for all temperatures examined, using air and oxygen. An example of the cell polarisation with air is shown later in Fig. 7, where typically peak power densities of 100 mW $cm^{-2}$ were obtained. Overall the cell polarisation reflects the positive and negative effects of increasing temperature on borohydride reactions and transport. Higher temperatures increase borohydride hydrolysis and borohydride crossover. At the same time when the temperature increases the reaction kinetics and the membrane conductivity increase, reducing the internal resistance of the system. The improvement in DBFC performance when the temperature is increased from 30 to 60 °C indicates that the latter factors outweigh the negative effects of increasing temperature.

Figure 4 shows the oxygen reduction polarisation characteristics measured in situ in the BDFC. There was little change in the cathode potential with current density over the current density range considered. The fall in potential from open circuit, for example at 50 °C, was around 30 mV. In addition the effect of an increase in temperature

**Table 3** Effect of temperature on cell power density performance for the DBFC using oxygen and air

| Temperature (°C) | Maximum power density for air (mW $cm^{-2}$) | Maximum power density for $O_2$ (mW $cm^{-2}$) |
|---|---|---|
| 30 | 66.67 | 77.78 |
| 40 | 78.33 | 94.17 |
| 50 | 91.39 | 125.00 |
| 60 | 105.00 | 149.33 |

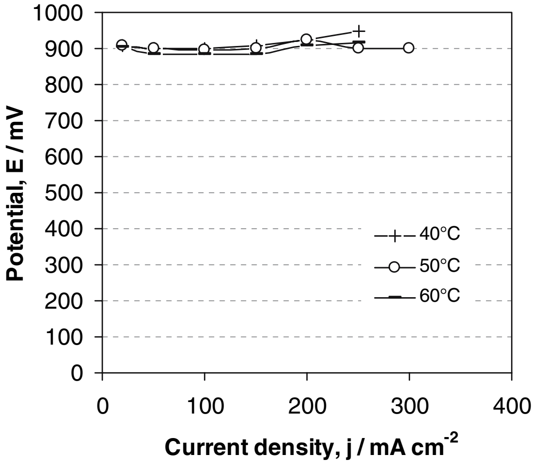

**Fig. 4** Effect of temperature on cathode oxygen reduction polarisation curves measured in the DBFC. Borohydride concentration 1.0 M in 1.0 M sodium hydroxide; solution anode flow rate 2.78 cm$^3$ min$^{-1}$, cathode flow rate 0.4 cm$^3$ min$^{-1}$, without back pressure

was not significant. This may be due to an increase in oxygen reduction kinetics being counteracted by an increase in the borohydride ion crossover, which tends to polarise the cathode during oxygen reduction. What is clear is that the major loss in cell performance was due to anode polarisation. Overall, these data demonstrate that the DBFC can deliver good power density and energy capacity even at ambient temperature [13].

Table 3 summarises the power density performance of the DBFC at different temperatures using air and oxygen. With oxygen the power density increased by a greater extent (approximately 100%) with an increase in temperature from 30 to 50 °C, compared to that with air (approximately 50%).

## 3.2 Influence of $NaBH_4$ concentration

The influence of $NaBH_4$ concentration on the anode and cell polarisations is shown in Figs. 5 and 6 respectively, for a temperature of 60 °C. Doubling the borohydride concentration to 2.0 M increased the maximum current density and increased the peak power density to 200 mW cm$^{-2}$. Such high power densities are particularly attractive for the borohydride fuel cell, operating under essentially ambient conditions. Using air as oxidant gave power densities between 85 and 140 mW cm$^{-2}$.

The increase in borohydride ion concentration only influenced the anode polarisation behaviour at the higher current densities and again the data were not consistent with a simple mass transport limitation of borohydride ion oxidation. At higher current densities we would expect that the local pH at the electrode surface would fall due to consumption of OH$^-$ ions, which would consequently cause catalytic decomposition of borohydride to hydrogen. When a higher borohydride concentration is used the DBFC would be expected to be more significantly affected by this pH change. This in part may counteract any possible benefits of an increase in concentration on borohydride ion oxidation kinetics. However, it is not known what, if any, effects there would be on the DBFC with local generation of hydrogen at the electrode solution interface.

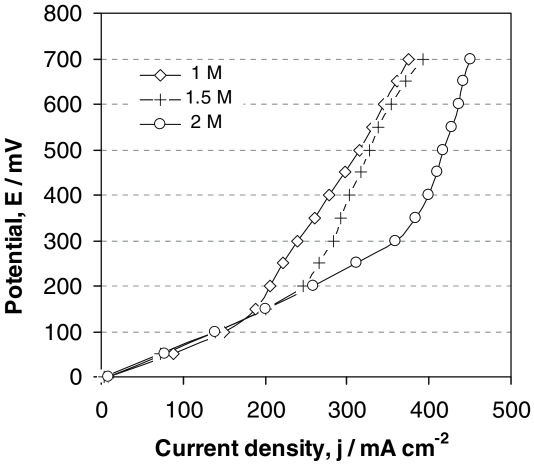

**Fig. 5** Effect of borohydride concentration on anode polarisation. 60 °C, 1.0 M sodium hydroxide; solution anode flow rate 2.78 cm$^3$ min$^{-1}$, cathode oxygen flow rate 0.4 cm$^3$ min$^{-1}$, without back pressure

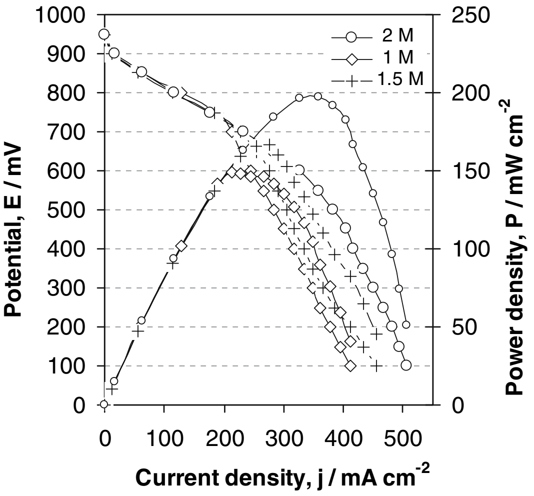

**Fig. 6** The effect of borohydride concentration on cell polarisation and power density with an oxygen cathode. 60 °C, 1.0 M sodium hydroxide; solution anode flow rate 2.78 cm$^3$ min$^{-1}$, cathode oxygen flow rate 0.4 cm$^3$ min$^{-1}$, without back pressure

## 3.3 Influence of NaOH concentration

The influence of sodium hydroxide concentration was examined over a small range, mainly because high concentrations would potentially have an adverse effect on the

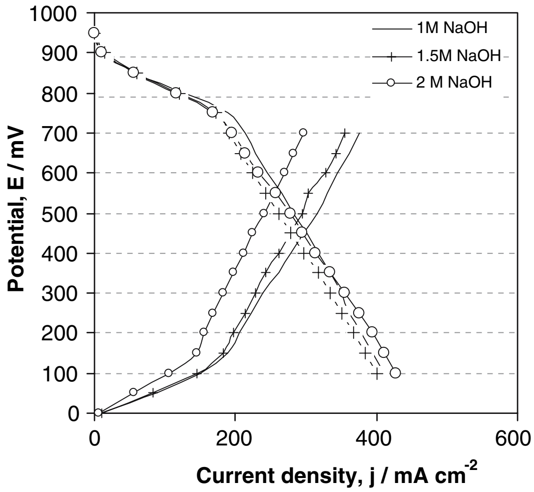

**Fig. 7** Effect of sodium hydroxide concentration on anode and cell polarisation curves. 60 °C, 1.0 M sodium borohydride; anode solution flow rate 2.78 $cm^3$ $min^{-1}$, cathode flow rate 0.4 $cm^3$ $min^{-1}$, without back pressure

stability of the anion exchange membrane. Increasing NaOH concentration has several effects; such as increasing the conductivity and reducing possible borohydride hydrolysis. There are also some negative effects, such as an increase in solution viscosity which decreases the mobility of borohydride ions in the anode catalyst layer [14].

Figure 7 shows the anode and cell polarisation curves obtained for different NaOH concentrations using air as oxidant. An increase in NaOH concentration produced inferior anode polarisation and cell performance. This behaviour suggests that the reduced mobility of the borohydride ions, produced by an increase in hydroxide ion concentration, may be a factor. However, it should also be established whether or not high $OH^-$ ion concentration benefits or inhibits the oxidation kinetics on Pt/Ru anodes. An additional influence may be the lower hydroxide ion transfer flux through the anion exchange membrane with the higher hydroxide ion concentration in the anode, i.e. a higher concentration difference impedes $OH^-$ ion transfer from the cathode to the anode.

Figure 8 shows the corresponding values of peak power density obtained for the DBFC working with air and oxygen. Values of power density were between 90 and 110 mW $cm^{-2}$ for air and 130–145 mW $cm^{-2}$ for oxygen; in the latter case the lowest value was obtained with a 1.5 M sodium hydroxide solution.

## 3.4 Influence of flow rate of $NaBH_4$ solution

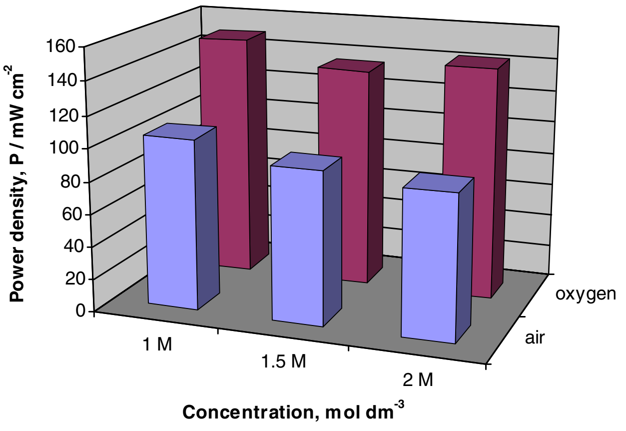

**Fig. 8** Effect of NaOH concentration on the maximum power density. 60 °C, 1.0 M sodium borohydride; anode flow rate 2.78 $cm^3$ $min^{-1}$, cathode flow rate 0.4 $cm^3$ $min^{-1}$, without back pressure

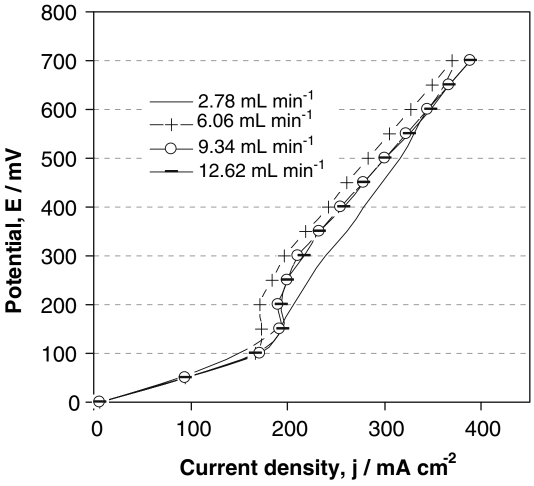

**Fig. 9** Effect of borohydride solution flow rate on anode polarisation. Borohydride concentration 1.0 M in 1.0 M sodium hydroxide, cathode flow rate 0.4 $cm^3$ $min^{-1}$, without back pressure, 60 °C

Figure 9 shows the anode polarisation curves obtained with different flow rates of borohydride solution in the anode from which we see that the flow rate did not have a major effect on anode performance. The limited influence of flow rate on anode performance was also reflected in the cell polarisation and power density performance, shown in Fig. 10. Although it may be possible to improve mass transport of borohydride to the anode by increasing flow rate, this effect is expected to be quite small as the major transport resistance, if any, would be in the catalyst diffusion layer where convective transport effects are largely absent. An indirect effect may come from a higher pressure in the anode side when the fuel flow rate is increased. This increase in pressure forces more water to pass from the anode to the cathode and potentially more borohydride, which may reduce the cell performance.

## 3.5 Durability test

Figure 11 shows the cell performance at a constant current of 100 mA $cm^{-2}$ recorded over a continuous operating

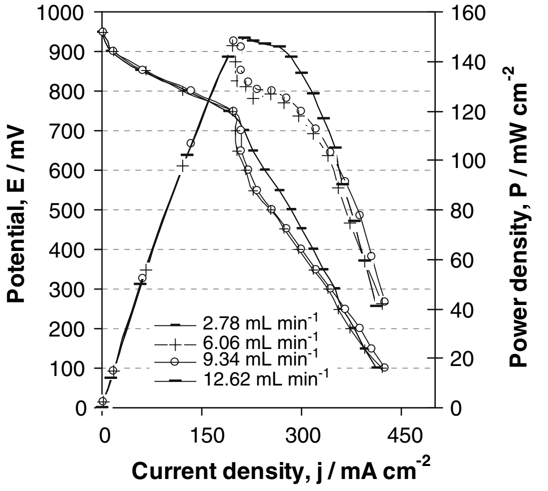

**Fig. 10** Effect of borohydride solution flow rate on cell polarisation and power density Borohydride concentration 1.0 M in 1.0 M sodium hydroxide, cathode flow rate 0.4 $cm^3$ $min^{-1}$, without back pressure, 60 °C

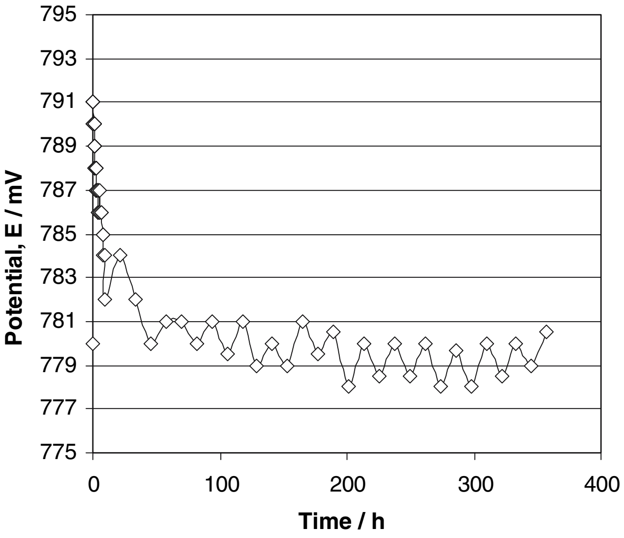

**Fig. 11** Stability test of the DBFC. Borohydride concentration 1.0 M in 1.0 M sodium hydroxide, cathode flow rate 0.4 $cm^3$ $min^{-1}$, without back pressure, 60 °C

period of 360 h. In this test, after an initial fall in potential of 10 mV over 50 h, the potential was quite stable with only a 2 mV fall over the remaining period.

## 4 Conclusions

The viability of a DBFC equipped with a anion exchange membrane and a Pt–Ru/C anode and Pt/C cathode has been demonstrated. The DBFC gave good performance; comparable with, and better than, many other DBFC systems and was stable over significant operating times. Power densities of 200 mW $cm^{-2}$ have been obtained using ambient oxygen cathodes at medium temperatures. The performance of the DBFC was very good at conditions close to room temperature, using modest catalyst loadings, of 1 mg $cm^{-2}$ in the anode and cathode. The fuel cell performance shows some dependence on sodium hydroxide and borohydride solution concentrations. The effect of anode solution flow rate on performance is small and data indicate that low flow rates are suitable.

**Acknowledgement** The work was supported by a fellowship to N Duteanu from the EU Marie Curie Training site supported by contract number HPMT-CT-2001–00333.

## References

1. Lamy E, Belgsir J, Leger J (2001) J Appl Electrochem 31:799
2. Reeve RW, Christensen PA, Dickinson AJ, Hamnett A, Scott K (2000) Electrochim Acta 45:4237
3. Chu D, Jiang R (2002) Solid State Ionics 148:591
4. Peled E, Duvdevani T, Aharon A, Melman A (2001) Electrochem Solid State Lett 4:A38
5. Muller T, Urban PR, Holderich WF, Colbow KM, Zhang J, Wilkinson D. P (2000) J Electrochem Soc 147:4058
6. Beattie D, Basura VI, Holdcroft SJ (1999) Electroanal Chem 468:180
7. Jasinski R (1965) Electrochem Tech 3:40
8. Amendola SC, Onnerud P, Kelly MT, Petillo PJ, Sharp-Goldman SL, Binder MJ (1999) J Power Sources 84:130
9. Li ZP, Liu BH, Arai K, Asaba K, Suda S (2004) J Power Sources 126:28
10. Li ZP, Liu BH, Arai K, Asaba K, Suda S (2003) J Electrochem Soc 150:A868
11. Chen J, Matsuura T, Hori M (2004) J Power Sources 131:155
12. Yu EH, Scott K (2004) J Power Sources 137:248
13. Cheng H, Scott K (2006) J Power Sources 160:407
14. Ponce de Leon C, Walsh FC, Pletcher D, Browning DJ, Lakeman JB (2006) J Power Sources 155:172
15. Li P, Liu BH, Arai K, Suda S (2003) J Electrochem Soc 150(7):A868
16. Liu H, Li ZP, Arai K, Suda S (2005) Electrochim Acta 50:3719